ESA Contract No. 4000119143/16/NL/BJ/zk

Numerical simulations for spacecraft catastrophic disruption analysis

EXECUTIVE SUMMARY

Issue 1.0 – 2019-05-13

Prepared by:	Lorenzo Olivieri	CISAS
Contribution by:	Karl Dietrich Bunte	etamax
Revision by:	Alessandro Francesconi	CISAS

1 Introduction

At present, the largest part of the catalogued space debris population consists of fragments originated by accidental explosions of spacecraft and upper stages, but it is expected that hypervelocity collisions engaging large objects could become the primary source of new debris in the mid-term future. In this context, understanding the **physical processes involved in spacecraft collisions is crucial**, because these big impacts are one of the key drivers of the long-term evolution of the space debris population. In particular, **hypervelocity impacts resulting in the fragmentation of very significant parts of the colliding objects** and the subsequent production of new debris large enough to cause other critical blows are referred to as "catastrophic collisions". It is believed that **catastrophic impacts occur when the kinetic energy of the impactor is greater than 40 Joule per unit mass (in grams) of the target** (energy-to-mass ratio EMR>40 J/g).

Currently, empirical and semi-empirical breakup models are the most common means to provide detailed descriptions of fragments clouds originated by catastrophic collisions. On one hand, the most used empirical breakup tool is indeed the NASA Standard Breakup Model (SBM) [1][2]. However, the actual version of the NASA SBM is not able capture the complexity of the various possible impact scenarios, as they result from latest spacecraft designs, as well as the effects of impact point (e.g. collision on main body vs. collision on appendages). On the other hand, semi-empirical models combine mass, momentum, and energy conservation principles with empirically-derived relationships from laboratory test data and observations of orbital breakups. Semi-empirical approaches are chosen to create simple, fast-running models not requiring very comprehensive inputs; two remarkable examples of semi-empirical breakup models are provided by FAST [3][4] and IMPACT [5][6]. Other simulations approaches, e.g. based on the use of finite elements, discrete elements, hydrocodes, or combinations of these techniques, are still in infancy because of the complexity of the physical problem, the large scales involved, and, most critical, the massive computational effort requested to analyse collisions with large multipart objects such as entire satellites.

In this context, this document provides **a general description and first results of the Collision Simulation Tool** (CST), a new software developed in the framework of the ESA contract "Numerical simulations for spacecraft catastrophic disruption analysis". The CST makes possible to **model a large variety of collision scenarios** involving complex systems such as entire satellites with many design details included and different encounter configurations, and provides statistically accurate results **with a computational effort significantly lower than hydrocodes and other "full physics" methods**.

The remainder of this document is organized as follows. Section 2 explains the new modelling approach used in CST, including descriptions of the three core algorithms of the tool (breakup, structural response, and tracking). Section 3 describes the software framework in which the simulator core is embedded. Section 4 reports a first set of validation results with empirical data of ground-based experiments on simple targets and sub-scale satellites. Section 5 describes simulations on completely new impact events involving the ESA LOFT spacecraft, with impactors ranging from 1U to 48U CubeSats, and diverse encounter configurations. Conclusions are finally given in Section 6.

2 Collision Simulation Tool modelling approach

The CST employs a hybrid simulation strategy built on a combination of different methods addressing diverse phases of satellite collisions. It is recognized that these large impact events involve two separate damage modes, which develops with different time scales: (1) **a diffuse**

cascade fragmentation initiated at the impact point, affecting those spacecraft parts that are directly involved in the local collision process, and (2) **a global satellite collapse** consequent to the propagation of shock waves through components connections and along the structure. The choice of a hybrid simulation methodology aims at dealing with these different damage modes with a unified approach.

In the CST, colliding objects are modelled with a **coarse mesh of Macroscopic Elements** (nodes) representing major satellite parts **connected by structural links** to form a system-level net (gross discrete-elements mesh), see Fig. 1. **Macroscopic Elements represent spacecraft elementary building blocks**, such as plates, sandwich panels, joints, etc. The first damage mode (fragmentation) is addressed through the use of semi-empirical breakup models that are applied at the level of Macroscopic Elements, depending on impact point, elements materials, and geometry. The second damage mode (structural failure) is addressed through a discrete-elements-like simulation of the momentum transferred to Macroscopic Elements in the net and the energy dissipated inside the elements and through the links.
Based on this modelling concept, the **simulator core** of the CST is divided in three main parts: (1) the **ME Breakup Algorithm**, providing fragments size, velocity, and area-to-mass distributions for a variety of spacecraft building blocks; (2) the **Structural Response Algorithm**, calculating momentum transfer, energy dissipation, structural deformation, and fracture, and (3) the **Fragments Tracking Algorithm**, which follows the trajectories of new debris created in the early stages of the event and detects the resulting multiple secondary impacts on other satellite parts. These three algorithms are described in the following sub-sections.

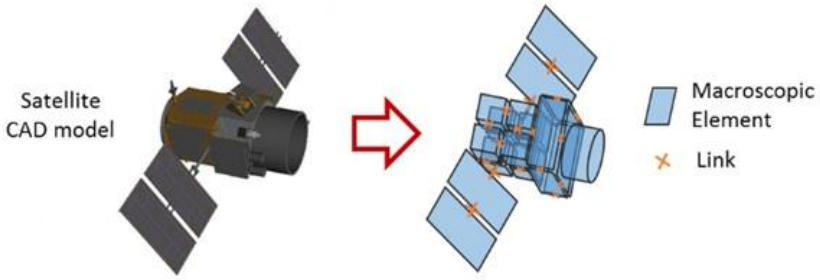

Fig. 1. Example of satellite model: net of Macroscopic Elements connected through links

2.1 Breakup Algorithm

The Breakup Algorithm calculates fragments distributions in terms of debris number, mass, size (area-to-mass), and velocity vectors for those Macroscopic Elements where a given fragmentation threshold is exceeded. This threshold is based on an energy criterion and depends from the impact point and direction and from the geometric and physical properties of every single Macroscopic Element subjected to impact.
The algorithm models the transition from local damage to catastrophic disruption by defining the MEs volumes damaged by impacts. Once such volumes are known, they are filled with fragments of given size and shape using an approach similar to that employed in computer graphics for the gaming and the movie industry [7] that involves the generation of pre-determined Voronoi fragmentation patterns. In fact, using available empirical data (e.g.: [8][9]), fragmentation patterns can be adapted to different impact conditions in order to produce fragments distributions representative of real hypervelocity impact events.
Finally, when fragments size distributions are known, velocity is calculated for each fragment with an approach similar to that used by the mentioned FAST tool.

2.2 Structural Response Algorithm

The Structural Response Algorithm simulates the global behaviour of the spacecraft structure subjected to transient loading. This is done through the integration of a set of differential equations that describe the dynamics of the nodes of the Macroscopic Elements net representing the satellite model. These nodes are subjected to impact forces provided by the primary collision and multiple hits of secondary fragments produced by the Breakup Algorithm, as well as internal actions consequent to the deformation of links between elements. These links describe the system structural continuity and their properties determine the large-scale response of the whole net, including the momentum and energy transferred to each ME, the energy dissipation, the net deformation, the possible rupture of joints, and the elements separation. All links are modelled following ECSS [10][11] and EUROCODES [12] norms for structural junctions.

2.3 Tracking Algorithm

In a typical collision event the total impact energy is not instantaneously transmitted from the impactor to the target, but it is rather transferred gradually as the two bodies penetrate each other and secondary fragments hit other satellite parts in their flight path. For this reason, the CST has been provided with the capability of modelling the progressive engagement of the colliding objects as well as the multiplicity of secondary impacts against intact macroscopic elements. This “chain reaction” is addressed by propagating the motion of fragments whose size and/or energy exceeds a certain threshold, while small and less energetic debris are collectively included in an expanding cloud of dust.

3 CST Framework

The **CST simulator core** is **embedded in a software framework**, which comes with a modern graphical user interface for creating collision geometries and executing the simulation. As shown in Fig. 2, the interface contains the **project explorer** for generating and overviewing different simulation projects, the **3D viewer** for visualising ME as well as CAD models, and three **editors for defining ME, Link, and material parameters**.

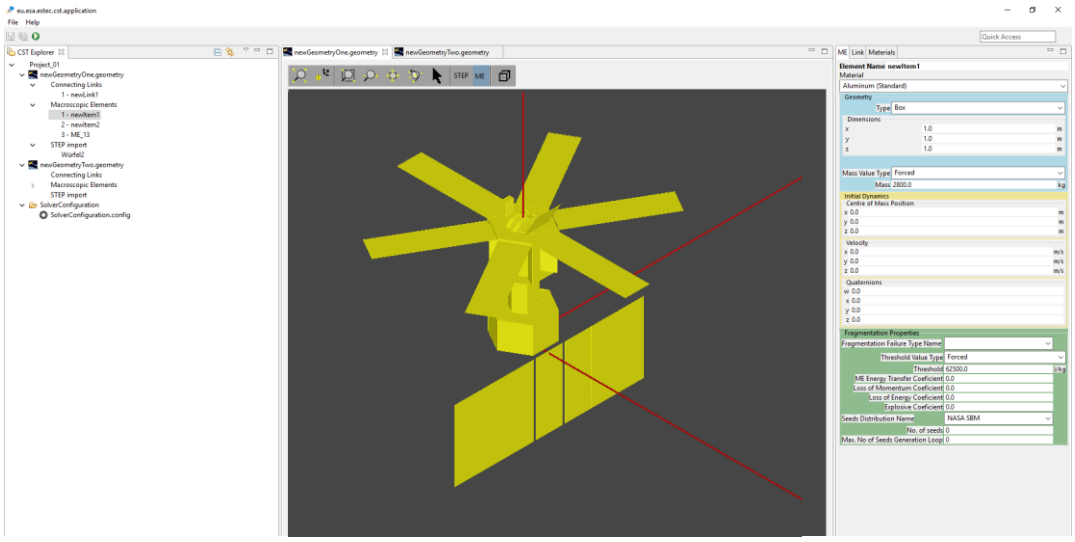

Fig. 2. CST GUI

In particular, the framework provides the means for: (1) creating collision simulation projects, (2) generating ME models from scratch or importing CAD models, automatically reducing them to a reasonable level of detail based on user defined thresholds and semi-automatically converting them to equivalent ME models by means of assigning basic shape types to mostly complex CAD

objects, (3) the definition of simulation and post processing parameters and the generation of tabled output and 2D diagrams for each simulation step.
To complete the ME model for the simulation, the user can edit the generated MEs, needs to define the links between MEs and to specify the material properties of the MEs. For this purpose, the framework also provides a Material Editor which enables the user to define and include new materials besides the available list of standard materials.

4 CST validation

The first validation of the software was done against empirical results from **ground-based impact tests on simple targets** (plates and Whipple Shields) as well as **sub-scale satellite models**.

4.1 Simple targets

Validation with simple targets has involved ground-based impact tests on single plates and Whipple Shields. In the first case, comparison between test data and CST results has been referred to both crater/hole size in the plate and, when available, fragments distributions in terms characteristic length and area-to-mass ratio. In the second case, the comparison has been limited to ballistic limit predictions.

4.1.1 Aluminium plates

CST validation with simple Aluminium plates was performed with reference to the dataset published by Nishida et al [8]. This dataset reports **crater size measurements and fragments size and normalized area distributions** from laboratory impacts on aluminium plates 30 mm thick. Spherical aluminium projectiles have diameter in the range 1.6 – 7.0 mm and velocity from 1.8 to 6.8 km/s. Test data and CST simulation results are presented for craters size in Table 1; fragments size and area distributions are plotted in Fig. 3 for one experiment (N7), as example. The **root mean square deviations of the CST curves** with respect to empirical data **are 22% and 39%, respectively for size and fragments area distributions**.

Table 1. CST validation with Aluminium simple plates using empirical data published in [8].

Test ID	d_{proj} (mm)	v_{proj} (km/s)	D_{crat}* (mm)	D_{crat}^{+} (mm)	Error (%)
N5	3.2	3.01	7.76	7.51	3.22
N6	1.6	3.09	3.85	3.82	0.78
N7	3.2	4.14	9.25	9.29	-0.43
N8	1.6	4.06	4.65	4.59	1.29
N9	3.2	6.62	12.52	12.71	-1.52
N10	1.6	6.75	6.18	6.44	-4.21

** Empirical result*

+ CST simulation

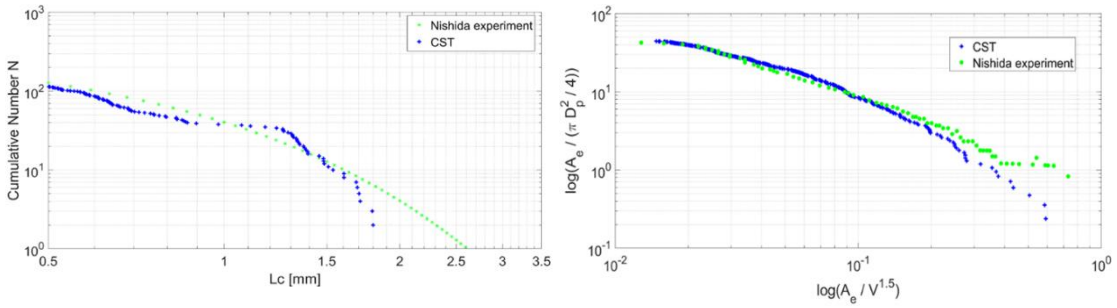

Fig. 3. Test N7: comparison between experimental and numerical fragments characteristic length distributions (top) and fragments normalized area distributions (bottom)

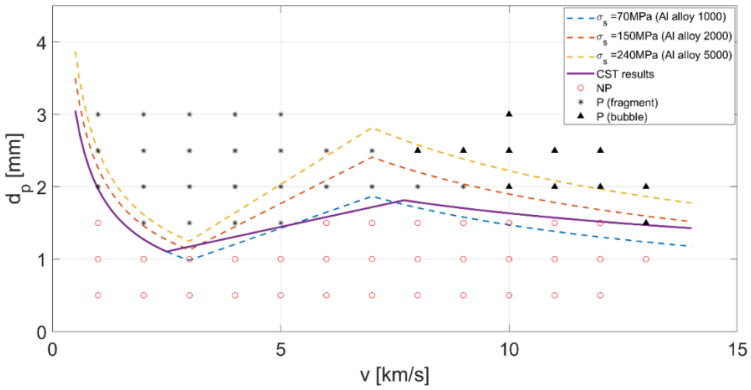

Fig. 4. Whipple Shield BLE calculated with CST (solid line) and with the Christiansen BLE (dashed lines). Each marker represents a CST simulation.

4.1.2 Whipple Shields

When shields are concerned, laboratory tests are usually focused on the study of **perforation and ballistic limit** and hence detailed information of empirical fragments distributions is normally missing. For this reason, validation was done through comparison of the Ballistic Limit Equation (BLE) obtained with the CST with the classic Christiansen's BLE for this type of shields [13]. An example of comparison is given in Fig. 4, with reference to a Whipple Shield composed by Aluminium bumper plate and back-wall of equal thickness (t_b=t_w=1.2 mm), separated by a standoff distance of S=100 mm. Solid markers (stars and triangles) and empty markers respectively represent perforation and non-perforation, as predicted by CST. Dashed lines are ballistic limit curves calculated with the Christiansen equation, and the solid line is the curve predicted by CST. Three types of failure modes were detected on the back wall: (1) individual fragments puncture (P-fragment in the figure), (2) debris "bubble" distributed load (P-bubble in the figure), and (3) combination of the two above. The total CPU time for the 50 simulations reported in Fig. 4 was about 0.5 hours (using a Xeon E5 2640V4 32 GB with 10 cores).

4.2 Sub-scale satellite mock-ups

In recent years some impact tests have been performed on both full-scale and sub-scale satellite mock-ups, and these experiments come with more useful information on fragments characteristic length and area-to-mass distributions. Thanks to these tests, the CST has been also validated against published empirical data related to a **nearly catastrophic collision on sub-scale satellite mock-ups.** An example is given in the paper by Lan et al [14], where laboratory tests are reported on cubic satellites made of Al-alloy plates and Al-alloy boxes, with side length = 40 cm and mass from 7295 g to 13100 g, impacted by 97 g Al-alloy blunt cone projectiles with 41 mm of bottom diameter and 58 mm length, from 3 to 3.6 km/s (see Fig.5)).

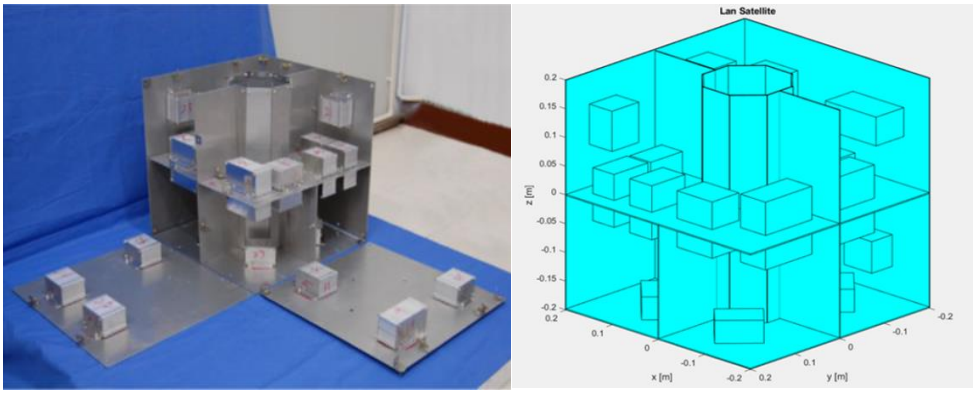

Fig. 5. Lan Satellite [14] and its CST model.

CST results are presented for a test case with projectile mass and velocity equal to 97 grams and 3.6 km/s, leading to an EMR=48.2 J/g, just above the classic 40 J/g threshold. The laboratory experiment in this case did not result in the complete spacecraft fragmentation, even though a significant satellite portion was disintegrated. A comparison between experimental results, CST results and NASA SBM is presented in Fig.6, respectively in terms of fragments characteristic length (left) and area-to-mass distributions (right).
The total CPU time for this simulation was about 4 hours (using a Xeon E5 2640V4 32 GB with 10 cores).

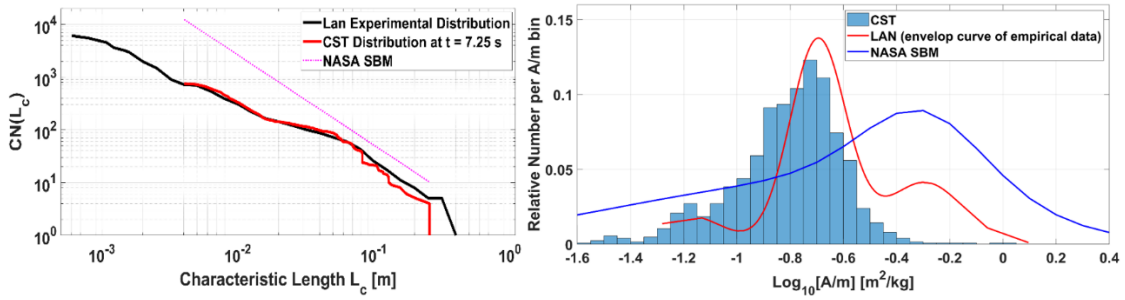

Fig. 6. Fragments characteristic length (left) and area-to-mass (right) cumulative distributions: comparison between experimental data, CST results and NASA SBM.

5 CST results with LOFT spacecraft

CST was finally evaluated versus its capability to simulate completely new impact events involving modern satellites. In this framework, the main focus was the **response of the ESA LOFT spacecraft** (Fig. 7, CAD and CST model) **to various types of collisions** (see Table 2) with impactors ranging from 1U to 48U CubeSats (EMR from ~3 to ~270 J/kg), and diverse encounter configurations such as impact on center of mass and impact on appendages.

Fig. 8 presents a summary of results, in terms of characteristic length distributions, for the first six LOFT test cases (LOFT1 to LOFT6). Simulation results are compared to the NASA SBM (catastrophic, and sub-catastrophic for plate, 1U CubeSat and 12U CubeSat impactors).

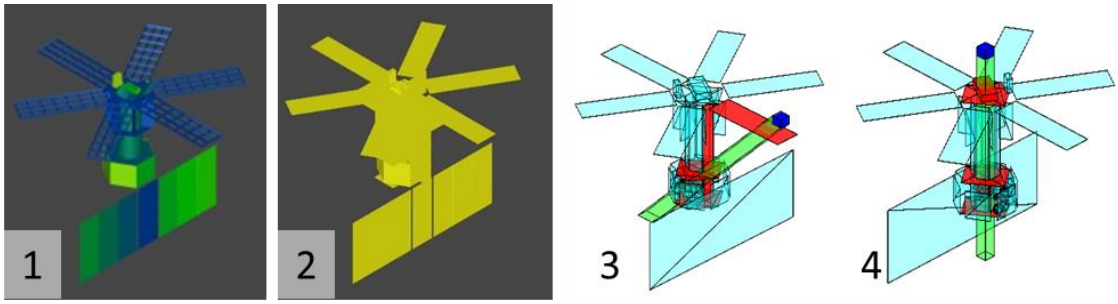

Fig. 7. LOFT satellite: CAD model (1), semi-automatic CST import (2), and cases LOFT7 (3) and LOFT8 (4)

Table 2: CST evaluation cases on the LOFT spacecraft.

Test ID	Impactor	Impact configuration
LOFT1	Al-alloy rectangular plate, mass=0.110 kg Plate size: 0.1 x 0.1 x 0.04 m^3 Relative velocity: 11 km/s, EMR: ~3 J/g.	Impactor plate hitting on edge the geometric centre of the LOFT main body. Impact angle: 0°.
LOFT2	Al-alloy 1U CubeSat, mass=1.0 kg CubeSat size: 0.1 x 0.1 x 0.1 m^3 Relative velocity: 11 km/s, EMR: ~28 J/g.	Impactor hitting the geometric centre of the LOFT main body, with face parallel to the satellite face. Impact angle: 0°.

LOFT3	Al-alloy 12U CubeSat, mass=12.0 kg CubeSat size: 0.2 x 0.2 x 0.3 m^3 Relative velocity: 10 km/s, EMR:~275 J/g.	As in case LOFT2.
LOFT4	As in case LOFT3	As in case LOFT2, but impact point is moved to reduce the Impactor/target overlap to 20% of the projected cross sections.
LOFT5	As in case LOFT3	Impactor hitting one detector panel, with free path towards space after impact. Impact angle: 45°
LOFT6	As in case LOFT3	Impactor hitting one detector panel, pointing towards the centre of the LOFT main body. Impact angle: 45°
LOFT7	Al-alloy 48U CubeSat, mass=40.0 kg. Impactor size: 0.4 x 0.4 x 0.3 m^3 Relative velocity: 5.5 km/s, EMR:~272 J/g.	Impactor hitting one detector panel, pointing towards the centre of the propellant tank in the LOFT main body. Impact angle: 45°
LOFT8	Same as LOFT 7.	Impactor vertically hitting the LOFT main body from top to bottom, with velocity vector corresponding to the axis of the LOFT cylinder. Impact angle: 0°.

It is shown that all events (LOFT1-LOFT6) produce fragments distributions closer to the corresponding NASA SBM sub-catastrophic lines than the catastrophic one, even for collisions with EMR >> 40 J/g. This indicates that **the classic EMR criterion is not adequate to capture the variability of all possible collision scenarios**. In fact, for a given EMR, the impact consequences may exhibit remarkable variations for different combinations of impactor size and velocity, and the same EMR can produce different damage if the impact point is changed (this is related to the objects mass involved in the collision). Furthermore, it is observed that **the NASA SBM may overestimate significantly the real fragments distributions in many cases, where impacts are not central and the ratio between impactor size and target size is small**.

These arguments are confirmed in the two last test cases (LOFT7 and LOFT8), where impactors are significantly larger than in LOFT3-LOFT6 (48U instead of 12U), but the EMR and total mass (impactor + target) are nearly the same as before (~272 J/g >> 40 J/g). In these cases, according to the NASA SBM, LOFT7 and LOFT8 should result in catastrophic events with nearly the same characteristic length distributions of fragments from other collisions with same EMR. However, simulations results (Fig. 7) highlight a quite significant increase of the fragments number from LOFT6 to LOFT8, and this is related to changes of the impactor cross section and the impact point, leading in both cases to **more mass involved in the collision process**.

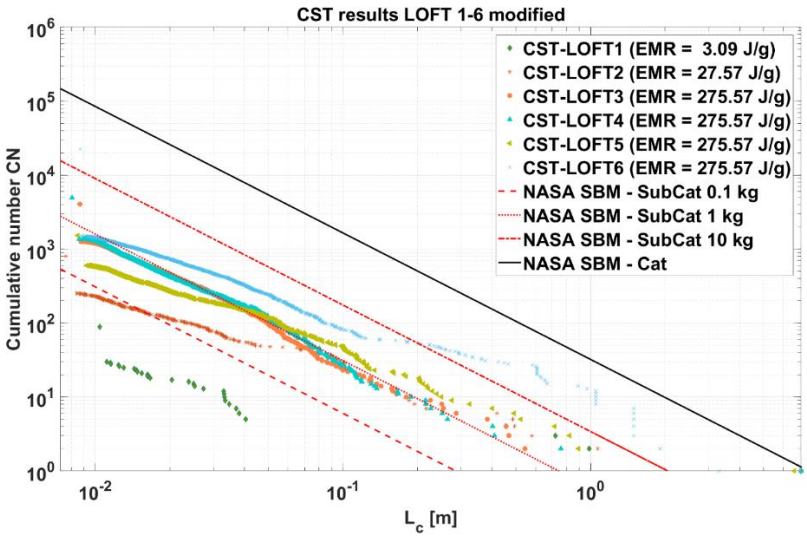

Fig. 8. Fragments characteristic length distributions for all LOFT cases. NASA SBM catastrophic and sub-catastrophic curves are also reported.

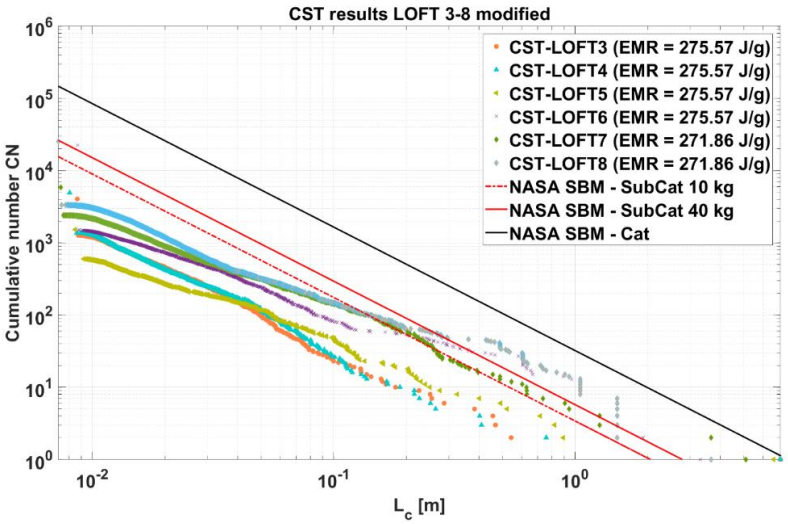

Fig. 9. Fragments characteristic length distributions for LOFT3-LOFT8 cases (all simulations with similar EMR and total mass). NASA SBM catastrophic and sub-catastrophic curves are also reported.

Based on these observations, a possible correction of the NASA SBM has been proposed which incorporates the objects mass fraction actually involved in the collision. This parameter could be related to the impactor/target cross-sectional overlap and to the impactor/target physical properties (e.g. densely packed or light object). Preliminary results with this correction indicate that the new curves represent satisfactorily the simulations only "on average", not in the full range. In fact, the number of small fragments appears in general to be overestimated, while the number of large fragments seems to be underestimated. Further work is needed in this respect.

6 Conclusions

This document describes **a new software tool for simulating large orbital collisions involving satellites**, aiming to predict fragments distributions from catastrophic and sub-catastrophic events. The new tool, called CST, is built on a hybrid simulation methodology, which describes spacecraft as a net of macroscopic elements connected through structural joints. The key innovation of the tool is related to the use of semi-empirical break-up models, which are individually applied to those elements of the net that are involved in the collision. Based on these semi-empirical models, debris fragments are locally generated and propagated, eventually causing secondary and successive impacts to other satellite parts. In the meantime, forces exchanged between the elements in the net are modelled to simulate the global structural response of the system.

The most notable features of this new simulation approach are **the very low computational intensity and the high suitability to generalization**: with the focus on spacecraft elementary building blocks rather than the entire satellite as a whole, it becomes possible to easily simulate collisions on a large number of different satellite architectures, all built with different combinations of known elements (e.g. plates, sandwich panels, joints, etc.). Furthermore, the CST has the capacity to model several objects design details and encounter configurations (i.e. impactor/target overlap and relative orientation). This approach has therefore the potential to significantly simplify laboratory tests for catastrophic impacts, since complex impact experiments on large satellite models could be in part replaced by simpler impact tests on spacecraft elementary parts.

First validation results are presented, with reference to empirical impact test data on simple plates, Whipple Shields, and a sub-scale satellite mock-up. In all these cases the CST demonstrated the capability of well reproducing the experiments outcomes.
Simulations on LOFT satellite show that that the classic EMR parameter is not sufficient to model the transition between sub-catastrophic and catastrophic impact in a certain variety of collision scenarios. In particular, same EMR can produce different damage if the impactor kinetic energy results from a different combination of impactor size and velocity (cross-sectional overlap effect), and same EMR can produce different damage if the impact point is changed (this is related to the objects mass involved in the collision). Furthermore, it is observed that the NASA SBM may overestimate significantly the real fragments distributions in many cases, where impacts are not central and the ratio between impactor size and target size is small.
In future, we plan to use CST for a large simulation campaign intended to systematically explore the key parameters of satellites collisions, with the aim of improving the accuracy of currently available breakup models, thus increasing the reliability of long-term debris environment predictions.

References

[1] R.C. Reynolds, et al. NASA Standard Breakup Model 1998 Revision, LMSMSS-32532, Lockheed Martin Space Mission Systems and Services, 1998.
[2] N.L. Johnson, P.H. Krisko, J.C. Liou, P.D. Anz-Meador PD (2001). NASA's New Breakup Model of EVOLVE 4.0. Adv. Space Res. 28(9), 1377-1384
[3] D. McKnight, et al. Fragmentation Algorithms for Strategic and Theater Targets (FASTT) Empirical Breakup Model. DNA-TR-94-104, 1994.
[4] D. McKnight, et al. Refined algorithms for structural breakup due to hypervelocity impact, Int. J. Impact Engng 17 (1995), 547-558
[5] M.E. Sorge. Satellite fragmentation modelling with IMPACT. In: Proc. AIAA/AAS Astrodynamics Specialist Conference and Exhibit, Hawaii, USA, 2008.
[6] M.E. Sorge, D.L. Mains. IMPACT fragmentation model developments, Acta Astronautica 126 (2016), 40-46.
[7] D. Frerichs, et al. A survey on object deformation and decomposition in computer graphics, Computers &Graphics 52 (2015), 18–32.
[8] M. Nishida, et al. Scaling laws for size distribution of fragments resulting from hypervelocity impacts of aluminum alloy spherical projectiles on thick aluminum alloy targets: Effects of impact velocity and projectile diameter. International Journal of Impact Engineering 109 (2017), 400-407.
[9] Nishida M, et al. (2013). Ejecta size distribution resulting from hypervelocity impact of spherical projectiles on CFRP laminates. Procedia Engineering, 58, 533-542.
[10] ECSS-E-HB-32-23A: Threaded fasteners handbook
[11] ECSS-E-HB-32-21A: Adhesive bonding handbook
[12] EN 1993-1-8:2005/AC: Eurocode 3: Design of steel structures - Part 1-8: Design of joints (2009)
[13] E.L. Christiansen, J.H. Kerr. Ballistic limit equations for spacecraft shielding. Int. J Impact Engng 26/1-10 (2001), 93-104.
[14] S. Lan, et al. Debris area distribution of spacecraft under hypervelocity impact. Acta Astronautica 105 (2014), 75–81.